PHYSICAL REVIEW B **80**, 161104(R) (2009)

Continuous metal-insulator transition of the antiferromagnetic perovskite $NaOsO_3$

Y. G. Shi,[1,2] Y. F. Guo,[1,2] S. Yu,[3] M. Arai,[4] A. A. Belik,[1,2] A. Sato,[5] K. Yamaura,[2,3,*] E. Takayama-Muromachi,[1,2,3] H. F. Tian,[6] H. X. Yang,[6] J. Q. Li,[6] T. Varga,[7] J. F. Mitchell,[7] and S. Okamoto[8]

[1]*International Center for Materials Nanoarchitectonics (MANA), National Institute for Materials Science, 1–1 Namiki, Tsukuba, Ibaraki 305–0044, Japan*

[2]*JST, Transformative Research-Project on Iron Pnictides (TRIP), 5 Sanbancho, chiyoda-ku, Tokyo 102–0075, Japan*

[3]*Superconducting Materials Center, National Institute for Materials Science, 1-1 Namiki, Tsukuba, Ibaraki 305-0044, Japan*

[4]*Computational Materials Science Center, National Institute for Materials Science, 1-1 Namiki, Tsukuba, Ibaraki 305-0044, Japan*

[5]*Materials Analysis Station, National Institute for Materials Science, 1-1 Namiki, Tsukuba, Ibaraki 305-0044, Japan*

[6]*Beijing National Laboratory for Condensed Matter Physics, Institute of Physics, Chinese Academy of Sciences, Beijing 100190, China*

[7]*Materials Science Division, Argonne National Laboratory, 9700 South Cass Avenue, Argonne, Illinois 60439, USA*

[8]*Materials Science and Technology Division, Oak Ridge National Laboratory, Oak Ridge, Tennessee 37831, USA*

(Received 28 August 2009; published 23 October 2009; corrected 28 October 2009)

The perovskite $NaOsO_3$ shows a Curie-Weiss metallic nature at high temperature and suddenly goes into an antiferromagnetically insulating state at 410 K on cooling. Electronic specific heat at the low-temperature limit is absent, indicating that the band gap fully opens. *In situ* observation in electron microscopy undetected any lattice anomalies in the vicinity of the transition temperature. It is most likely that the antiferromagnetic correlation plays an essential role in the gap opening.

DOI: 10.1103/PhysRevB.80.161104 PACS number(s): 71.30.+h, 72.80.Ga

Metal-insulator transition (MIT) is a central topic of condensed-matter science for more than half a century, and it still attracts intense attentions because it underlies key principles of correlated electron science. Chronologically, a principal idea was proposed by Mott in 1940s and by Hubbard in 1960s, suggesting that strong Coulomb interaction in half filling opens a gap at the Fermi energy (E_F), turning the conducting state into an insulating state, regardless of the presence of magnetic correlations.[1,2] Alternatively, Slater suggested in 1950s that antiferromagnetic (AF) order alone can open a gap in the half-filled state regardless of the magnitude of the Coulomb interaction.[3] Experimentally, many numbers of conductors were found to show MIT, which seems to be well characterized in the above schemes.[4] Regarding the AF correlation-induced MIT, most discoveries were attained on low-dimensional conductors and fairly few were on three-dimensional (3D) conductors. Generally, a 3D conductor causes only a small fraction of changes in its electronic structure through the AF ordering, resulting in robust conductivity such as found in Cr.[5] In this context, the 3D conductors $Cd_2Os_2O_7$ (Refs. 6 and 7) and $Ln_2Ir_2O_7$ (Ref. 8) are outstanding because of those continuous AF MITs.

So-far studies on $Cd_2Os_2O_7$ suggested that the continuous MIT at 226 K can be characterized in terms of the AF correlation,[6,7] although inherent magnetic frustration due to the pyrochlore lattice certainly complicates the MIT. The origin of the MIT of $Ln_2Ir_2O_7$ might include the magnetic frustration somewhat.[8] It appears that the AF 3D MIT needs to be studied further. It is thus highly desirable to investigate an AF 3D MIT that is less relevant to the magnetic frustration.

We report a perovskite oxide showing a continuous MIT. The perovskite $NaOsO_3$ has the octahedral environment of $Os^{5+}O_6$ so that the electronic configuration is $5d^3$, suggesting that the t_{2g} band is nearly half filling. $NaOsO_3$ shows a Curie-Weiss (CW) metallic nature and abruptly turns to an AF insulator at 410 K on cooling. It is notable that an AF 3D MIT appears on the perovskite lattice rather than the pyrochlore lattice. Because $NaOsO_3$ is expected to be less relevant to the magnetic frustration unlike the isoelectronic $Cd_2Os_2O_7$ and charge ordering is absent over the MIT of $NaOsO_3$, the perovskite is therefore significant to provide valuable opportunities to deepen our understanding of AF 3D MIT.

Crystal of $NaOsO_3$ grew up in a high-pressure apparatus that is capable of maintaining 6 GPa pressure during heating at 1700 °C for 2.5 h. The starting materials were Na_2O_2 (97%, Sigma-Aldrich) and OsO_2 (Os-84.0%, Alfa Aesar), and those were sealed in a Pt capsule at 15 mol % Na-rich stoichiometry with 0.1 mol of NaCl (99.99%, Rare Metallic Co.) per f.u. After the heating, the capsule was quenched in the press to ambient temperature before releasing the pressure. We prepared a polycrystalline sample as well by heating at 1200 °C for 1 h in the press without using NaCl. A photograph of a selected crystal is shown in Fig. 1(a). The samples were rinsed in water in a sonic bath for 2–3 min several times to remove residual ingredients, followed by

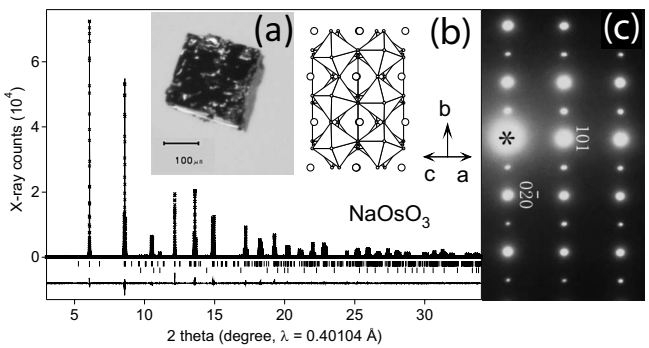

FIG. 1. (a) Photograph of a crystal of $NaOsO_3$ and (b) the Rietveld analysis of the synchrotron XRD profile for $NaOsO_3$. Cross markers and solid lines show the observed and calculated XRD profiles, respectively, and the difference is shown at the bottom. The positions of Bragg reflections are marked by ticks (lower ticks are for the impurity OsO_2). The inset is a structure view of $NaOsO_3$. (c) SAED pattern taken along [10–1] zone axis at room temperature.

drying in air at 140 °C for 10 min. The sample quality was checked by a powder x-ray diffraction (XRD) method using Cu $K\alpha$ radiation in RINT 2200V, RIGAKU, confirming the absence of impurities. We should note that preliminary samples prepared without excess Na_2O_2 were found to contain nontrivial amount of OsO_2. The crystal structure of $NaOsO_3$ was studied by a Rietveld method with powder synchrotron XRD data collected on the X-ray Operations and Research Beamline at the Advanced Photon Source, Argonne National Laboratory. The incident beam was monochromatized at $\lambda = 0.401\ 036$ Å. The Rietveld analysis was carried out by the program RIETAN-2000.[9]

A selected crystal of $NaOsO_3$ was examined in electron probe microanalysis (JXA-8500F, JEOL), finding the absence of contaminations such as Pt. The mean metal ratio at five points in the sole crystal was Na/Os=1.14(2), suggesting that a small amount of Na is possibly incorporated in the crystal. Crystals were studied by a selected area electron diffraction (SAED) method between room temperature and 600 K in a transmission electron microscope operated at 200 kV (Tecnai-F20, Philips Electron Optics). The electrical resistivity (ρ) of a selected crystal was measured by a van der Pauw method on the assumption that the charge transport of the crystal is isotropic in nature with a dc-gauge current of 0.1 mA between 2 and 330 K in Physical Properties Measurement System (PPMS), Quantum Design. Electrical contacts on the four corners of the crystal were prepared by gold wires and a silver paste. The limited size of the crystal did not allow us to estimate the actual degree of the charge transport anisotropy. ρ measurements between 300 and 550 K were conducted in a laboratory-made apparatus. The Hall coefficient (R_H) was measured by rotating the crystal by 180° in a magnetic field of 50 kOe in PPMS between 25 and 400 K.

The specific heat (C_p) was measured by a time-relaxation method using the powder sample (compressed) in PPMS between 2 and 300 K. Differential scanning calorimetry (DSC) was conducted in DSC1 STAR^e System, Mettler Toledo, between 300 and 440 K at heating rates of 0.5, 2, 5, 10, and 20 K/min. The magnetic susceptibility (χ) and the isothermal magnetization were measured using multiple single crystals randomly oriented in a sample holder (~20 pieces, 8.1 mg in total) in Magnetic Properties Measurement System, Quantum Design. The sample was cooled to 2 K without applying a magnetic field, and then warmed up to 300 K in a field of 50 kOe [zero-field cooling (ZFC)], followed by cooling to 2 K in the field [field cooling (FC)]. The measurement was again conducted between 300 and 600 K in an oven installed to the magnetometer.

Figure 1(b) shows the synchrotron XRD pattern with the analysis result.[10] A structure model with the space group *Pnma*, which is often observed for perovskite oxides, was found to reasonably fit to the pattern. The *R* factors and the difference curve in Fig. 1(b) indicate the high quality of the solution. The overall structure view is drawn in Fig. 1(b). Based on the result, we investigated the local coordination of Os. We found that it is fairly isotropic: variation of the six bond distances between Os and O is smaller than 0.4% of the longest 1.946(1) Å bond, and the O-Os-O angles are 90.7°, 89.9°, and 90.1°, being fairly close to the right angle. Besides, in order to alternatively confirm the solution quality, the bond valence sum of the atoms in the cell was calculated:[11,12] 4.92(Os), in reasonable agreement with the formal valence of Os and 1.40(Na), which is fairly obtained.

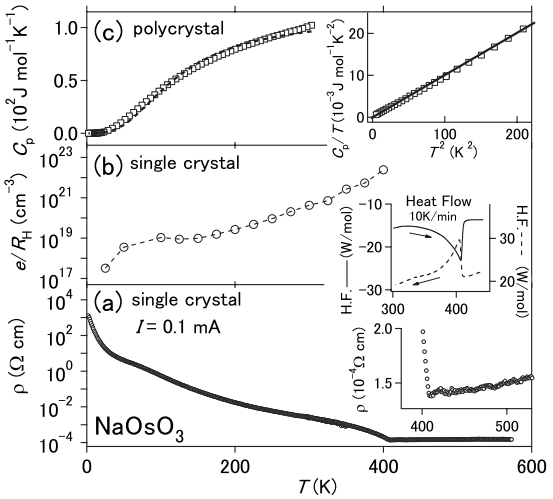

FIG. 2. T dependence of (a) ρ, (b) R_H, and (c) C_p of $NaOsO_3$. The inset shows an expansion of ρ vs T, DSC curves, and C_p/T vs T^2 (solid line is a fit to the data) at the low-temperature limit. The data were measured by a van der Pauw method on the assumption that the charge transport of the crystal is isotropic in nature.

We also studied the perovskite lattice by a SAED method and found that all diffraction spots at room temperature are distributed in accord with the *Pnma* model; in short the $\sqrt{2}a_p \times 2a_p \times \sqrt{2}a_p$ (a_p: primitive cell constant) order was clearly confirmed. The superstructure is due to the cooperative rotation and tilting of the OsO_6 octahedra as in the $GdFeO_3$-type perovskite.[13] Additional superstructure neither commensurate nor incommensurate was detected at room temperature. A selected SAED pattern is shown in Fig. 1(c). Besides, we carried out *in situ* heating in the microscope to test the appearance of a possible lattice anomaly over the MIT. However, no visible changes were detected to 600 K, excluding a major structure change and strong lattice-electron coupling in the vicinity of the MIT temperature. However, a possibility of structural distortions in local without symmetry change still remains, being investigated in future studies.

Figure 2(a) shows the temperature dependence of ρ of the single crystal $NaOsO_3$. The higher-temperature part shows a slightly positive slope around the resistivity of $\sim 1-2 \times 10^{-4}$ Ω cm, being consistent with an expected character for a metallic oxide. ρ suddenly jumps up at 410 K on cooling and continuously rises to 2 K over six orders of magnitude. It is notable that the warming and the cooling curves follow the same trace within an experimental accuracy, suggesting that the MIT is the second-order phase transition. The DSC confirmed the order of the transition (see the inset to Fig. 2), as the heat-flow-peak temperatures in cooling and heating are identical. The DSC measurements were repeated at different rates to extrapolate the result for 0 K/min, finding no shifts in the peak onsets and the peak positions.

In Fig. 2(b), the Hall number (e/R_H) steadily decreases with temperature decreasing beyond five orders of magni-

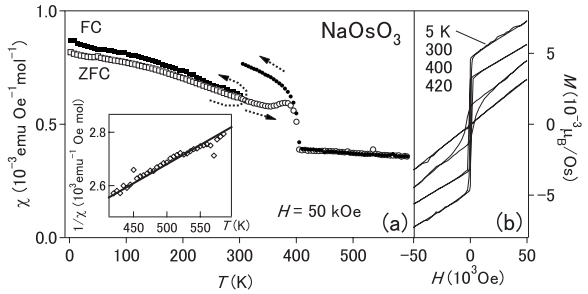

FIG. 3. (a) T dependence of χ of amount of single crystals of $NaOsO_3$, measured separately below (squares) and above (circles) 300 K. The inset shows an alternative plot of the data above 410 K. (b) Isothermal magnetization of $NaOsO_3$. The measurements were conducted on crystals randomly oriented in a sample holder.

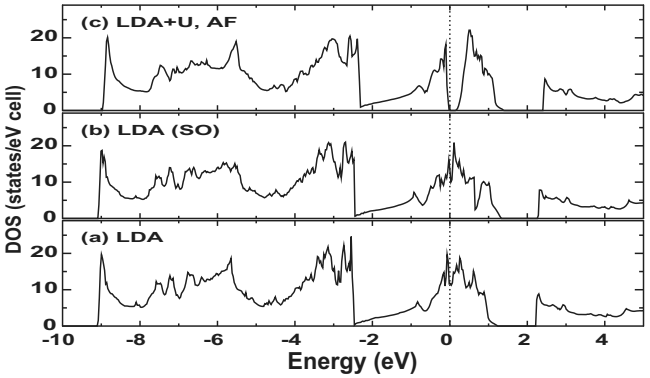

FIG. 4. (a) Nonmagnetic DOS of $NaOsO_3$ (b) with SO coupling. (c) AF DOS with U.

tude, indicating that the carrier density is reduced continuously by the gap opening. The carrier density measured at 400 K (the technical limit) corresponds to 1.31 holes per the primitive cell, indicating that $NaOsO_3$ has a sufficient amount of positively charged carriers. The estimated Hall mobility at 400 K is 1.3 $cm^2\ V^{-1}\ s^{-1}$, being not far from that for $Cd_2Os_2O_7$.[6] We also estimated the Hall mobilities at 200 and 25 K; they are 13.8 and 1.2 $cm^2\ V^{-1}\ s^{-1}$, respectively. It appears that the Hall mobility changes by one order of magnitude; however, the change is too small to account for the large ρ change beyond six orders of magnitude. We thus conclude that the MIT is not due to losing the charge mobility.

We measured the temperature dependence of C_p of $NaOsO_3$ in order to further study the MIT: C_p vs T is shown in Fig. 2(c). From 2 to 300 K, C_p changes rather monotonically without manifesting anomalies, suggesting the absence of additional transitions. To parametrize C_p, the curve was analyzed by the Debye model. The fit was conducted by a least-squares method and the best result (shown as a broken curve) yielded a Debye temperature (T_D) of 505(5) K and the number of vibrating modes per f.u. in the Debye model (n_D) is $0.882(6)\times 5$. Besides, the low-temperature part of C_p was analyzed using the approximated Debye model $C(T)/T=\beta T^2+\gamma$, where β and γ are a coefficient and the electronic-specific-heat coefficient, respectively [see the inset to Fig. 2(c)]. In accord with the model, the data changes linearly (<14 K), yielding a β of $9.83(5)\times 10^{-5}$ J $mol^{-1}\ K^{-4}$ and $\gamma=0.00(5)$ mJ $mol^{-1}\ K^{-2}$. We obtained a T_D of 462.4(8) K from β, where n_D was assumed to be 5. It appeared that γ is practically absent, suggesting that the electronic state is fully gaped at the low-temperature limit. For a comparison, γ estimated from the density of states (DOS) (without U, discussed later) is 7 mJ $mol^{-1}\ K^{-2}$, being distinguishable from the observed γ.

Figure 3(a) shows the temperature dependence of χ. First of all we should state that the discontinuous gap in the FC curve at 300 K is solely due to a technical matter regarding the heating attachment and does not entirely reflect the magnetism of the sample. Second, it is clear that χ vs T curves show a prominent anomaly at 410 K in the ZFC/FC conditions, indicating an establishment of a long-range magnetic order. We found that the magnetic transition is coincident with the MIT (ρ vs T). The isothermal magnetization in Fig. 3(b) displays the evolution of the magnetization over the transition. We found that the spontaneous magnetization is fairly small, $0.005\mu_B$/Os at 5 K; this corresponds to only 0.17% of the expected moment for $S=3/2$, indicating that the transition is weakly ferromagnetic (FM).

In order to further analyze the magnetic properties, we applied the CW law to the paramagnetic part (>410 K), as shown in the inset to Fig. 3(a). The analytical formula was $\chi(T)=N_A\mu_{eff}^2/3\pi(T-\Theta_W)$, where N_A is the Avogadro's constant and Θ_W is the Weiss temperature. The effective Bohr magneton (μ_{eff}) was estimated to be $2.71\mu_B$, being 70% of the expected moment for $S=3/2$. Θ_W was -1949 K, suggesting that AF interactions are strong and dominant in the spin system if the CW analysis provides a valid indication. The overall magnetic data including the CW analysis results thus suggest that $NaOsO_3$ undergoes an AF transition at 410 K accompanying the weak magnetization most likely due to the Dzyaloshinsky-Moriya interaction generated by the broken inversion symmetry.

We studied the electronic structure of $NaOsO_3$ using the local-density approximation (LDA) (Ref. 14) of density-functional theory.[15] We used the WIEN2K package,[16] which is based on a full-potential augmented-plane-wave method. Experimental lattice parameters and atomic coordinates were used with the atomic radii of 2.0, 1.8, and 1.7 a.u. for Na, Os, and O, respectively. The cutoff wave number K in interstitial region was set to $RK=7$, where R is the smallest atomic radius. The integration over Brillouin zone was performed by a tetrahedron method with 144 k points in the irreducible Brillouin zone (IBZ). For spin-polarized calculations, the convergence was checked with finer integration mesh points up to 468 k points in the IBZ.

The DOS is plotted in Fig. 4(a). The Os t_{2g} bands distribute between -2.5 and 1 eV, being wider than those for $Cd_2Os_2O_7$,[17] because frustration is absent in $NaOsO_3$. Reflecting the nominal configuration of Os^{5+} with $5d^3$, the calculated E_F lies near the center of Os t_{2g} bands and the total DOS shows the broad peak around E_F. Since the half-filled t_{2g} bands suggest instability of the nonmagnetic phase, we examined possible magnetic solutions within LDA. However, any stable solutions with FM or AF spin alignments were found. Besides, we further performed LDA calculations with spin-orbit (SO) coupling since they may affect qualitatively the electronic structure, as intensively discussed for

the 5*d* oxide Sr_2IrO_4.[18] Figure 4(b) shows the total DOS with SO coupling. As is common with $Cd_2Os_2O_7$,[19] the SO coupling indeed modifies the t_{2g}-band structure. However, E_F still locates at the vicinity of the broad peak with an almost comparable DOS, suggesting that the SO coupling plays an insignificant role in the gap opening in $NaOsO_3$ unlike what was found for Sr_2IrO_4.[20] Stable magnetic solutions with the SO coupling were unattained.

Afterward, we somehow obtained a stable magnetic solution by introducing a local coulomb interaction U as the Hubbard term in the LDA+U approximation. At a moderate U of 1 eV, a stable AF solution appeared with a small but finite energy gap as shown in Fig. 4(c), while attempts with FM spin alignments never resulted in a corresponding solution qualitatively and quantitatively. Thus, the results suggest that the AF correlation is highly significant to open the gap in $NaOsO_3$. It is also suggested that a picture with a large on-site U alone ($U \gg W$, where W is the bandwidth[1]) is too simple to account for the MIT of $NaOsO_3$.

The MIT of $NaOsO_3$ seems to be characterized by the degree of magnitude of AF correlation, as discussed in Ref. 19. The theoretical study using dynamical mean-field technique suggested that a gapped state in a half-filled electronic structure appears at the strong limit of the AF correlations, while a Mott transition is caused by the strong Coulomb repulsion regardless of the magnitude of magnetic correlations. In fact, magnetically weak materials such as V_2O_3 and much magnetic materials such as $NiS_{2-x}Se_x$ show different MIT features.[4] Regarding $NaOsO_3$, the MIT coincides with the AF transition; $NaOsO_3$ is thus close to the strong magnetic limit of the 3D MIT.[19] We believe that such a paramagnetic metal to AF insulator transition at finite temperature is of second order as we observed. Further discussion is left for future work.

On the other hand, a charge-order model was intensively discussed for the 3*d* perovskite $LnNiO_3$ (Refs. 20 and 21): the MIT features are however readily distinguishable from what we found for $NaOsO_3$. For instance, $SmNiO_3$ shows a large temperature gap between the MIT at 400 K and a subsequent magnetic transition at 220 K.[22] In addition, the magnetic transition in $SmNiO_3$ is coupled with lattice alteration probably due to ordering between the t_{2g} and e_g orbitals, while such a strong electron-lattice coupling is absent in $NaOsO_3$. It is thus reasonable to exclude the charge-order model from the framework of the MIT of $NaOsO_3$.

In summary, the perovskite $NaOsO_3$ shows a dramatic MIT at 410 K. The MIT nature is far different from what we observed for $LnNiO_3$ since it is associated with the magnetic ordering and is less relevant to the lattice anomaly. Furthermore, it is possibly different from the MIT nature of the isoelectrical $Cd_2Os_2O_7$ because the degree of magnetic frustration is highly reduced and the SO coupling is insignificant. The first-principles calculation suggests that the intense AF correlation (with small U) is the principal origin of the MIT of $NaOsO_3$. If the picture is true, $NaOsO_3$ is a "Slater insulator" in three dimensions, which can work at room temperature. Further studies toward the nature of the MIT and possible practical applications are in progress.

We thank D. Mandrus for valuable discussion, T. Kolodiazhnyi for the R_H measurement, and K. Kosuda for the EPMA. The use of the Advanced Photon Source was supported by the U.S. Department of Energy, Office of Science, Office of Basic Energy Sciences, under Contract No. DE-AC02-06CH11357. This research was supported in part by the WPI Initiative on Materials Nanoarchitectonics from MEXT, Japan and the Grants-in-Aid for Scientific Research (Grant No. 20360012) from JSPS. S.O. is supported by the Division of Materials Sciences and Engineering, Office of Basic Energy Sciences, U.S. Department of Energy.

*yamaura.kazunari@nims.go.jp

[1] N. F. Mott, Proc. Phys. Soc., London, Sect. A **62**, 416 (1949).
[2] J. Hubbard, Proc. R. Soc., London, Sect. A **276**, 238 (1963).
[3] J. C. Slater, Phys. Rev. **82**, 538 (1951).
[4] M. Imada, A. Fujimori, and Y. Tokura, Rev. Mod. Phys. **70**, 1039 (1998).
[5] E. Fawcett, Rev. Mod. Phys. **60**, 209 (1988).
[6] D. Mandrus, J. R. Thompson, R. Gaal, L. Forro, J. C. Bryan, B. C. Chakoumakos, L. M. Woods, B. C. Sales, R. S. Fishman, and V. Keppens, Phys. Rev. B **63**, 195104 (2001).
[7] W. J. Padilla, D. Mandrus, and D. N. Basov, Phys. Rev. B **66**, 035120 (2002).
[8] K. Matsuhira *et al.*, J. Phys. Soc. Jpn. **76**, 043706 (2007).
[9] F. Izumi and T. Ikeda, Mater. Sci. Forum **321-324**, 198 (2000).
[10] Na(4*c*), x=0.0328(5), y=0.25, z=−0.0065(7), B(Å^2)=1.00(4); Os(4*b*), 0, 0, 0.5, 0.277(3); O1(4*c*), 0.4834(10), 0.25, 0.0808(8), 0.77(7); O2(8*d*), 0.2881(5), 0.0394(4), 0.7112(5), 0.16(5); space group: *Pnma*; Z=4; a=5.384 20(1) Å, b=7.580 38(1) Å, c=5.328 17(1) Å, V=217.4654(6) Å^3; R_{wp}=12.54%, S=R_{wp}/R_e=2.07, R_F=2.09%.
[11] I. D. Brown, Acta Crystallogr., Sect. B: Struct. Crystallogr. Cryst. Chem. **33**, 1305 (1977).
[12] $R_0(Os^{5+})$=1.868 was used in the calculation; J. Yamaura, S. Yonezawa, Y. Muraoka, and Z. Hiroi, J. Solid State Chem. **179**, 336 (2006).
[13] S. Geller and E. A. Wood, Acta Crystallogr. **9**, 563 (1956).
[14] J. P. Perdew and Y. Wang, Phys. Rev. B **45**, 13244 (1992).
[15] P. Hohenberg and W. Kohn, Phys. Rev. **136**, B864 (1964).
[16] P. Blaha, K. Schwarz, G. K. H. Madsen, D. Kvasnicka, and J. Luitz, *WIEN2K: An Augmented Plane* Wave+Local *Orbitals Program for Calculating Crystal Properties* (Karlheinz Schwarz, Techn. Universitat Wien, Wien, Austria, 2001).
[17] D. J. Singh, P. Blaha, K. Schwarz, and J. O. Sofo, Phys. Rev. B **65**, 155109 (2002).
[18] B. J. Kim, Hosub Jin, S. J. Moon, J.-Y. Kim, B.-G. Park, C. S. Leem, Jaejun Yu, T. W. Noh, C. Kim, S.-J. Oh, J.-H. Park, V. Durairaj, G. Cao, and E. Rotenberg, Phys. Rev. Lett. **101**, 076402 (2008).
[19] R. Chitra and G. Kotliar, Phys. Rev. Lett. **83**, 2386 (1999).
[20] M. Medarde, M. T. Fernández-Díaz, and Ph. Lacorre, Phys. Rev. B **78**, 212101 (2008).
[21] C. Piamonteze, H. C. N. Tolentino, A. Y. Ramos, N. E. Massa, J. A. Alonso, M. J. Martinez-Lope, and M. T. Casais, Phys. Rev. B **71**, 012104 (2005).
[22] J. Perez-Cacho, J. Blasco, J. Garcıa, M. Castro, and J. Stankiewicz, J. Phys.: Condens. Matter **11**, 405 (1999).